Science of the Total Environment 906 (2024) 167498

Contents lists available at ScienceDirect

Science of the Total Environment

journal homepage: www.elsevier.com/locate/scitotenv

High-levels of toxic elements and radioactivity in an abandoned sulphur mine: Insights on the origin and associated environmental concerns

Matteo Giordani [a,*], Marco Taussi [a], Maria Assunta Meli [b], Carla Roselli [b], Giacomo Zambelli [c], Ivan Fagiolino [d], Michele Mattioli [a]

[a] Department of Pure and Applied Sciences, University of Urbino Carlo Bo, Urbino, Italy
[b] Department of Biomolecular Sciences, University of Urbino Carlo Bo, Urbino, Italy
[c] Radioprotection Expert, Protex Italia srl, Forlì, Italy
[d] C.S.A. Group Spa, Rimini, Italy

HIGHLIGHTS

- Fibrous epsomite in the Perticara mine shows high concentrations of ^{210}Po and ^{210}Pb.
- Bitumen contains ^{210}Po, while the host rock shows a slight anomaly of ^{40}K and ^{226}Ra.
- Water shows high amounts of Mn, Al, Fe, Pb and Mg.
- High concentrations of ^{222}Rn are present in the tunnel.
- Epsomite is able to capture radioactive elements in confined environments.

GRAPHICAL ABSTRACT

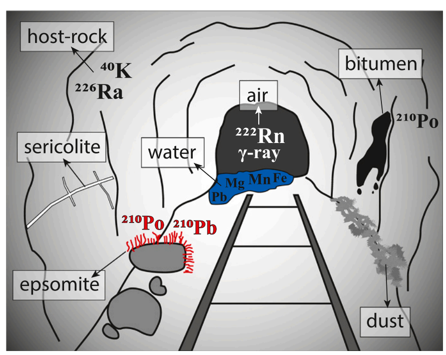

ARTICLE INFO

Editor: Daniel Alessi

Keywords:
Epsomite
^{210}Po
^{210}Pb
Radioactivity
PTEs
Gessoso-Solfifera formation
Sulphur mine

ABSTRACT

Natural fibrous epsomite crystals containing high amounts of toxic and radioactive elements have recently been discovered in the abandoned sulphur mine of Perticara (Italy). In the present study, all the different matrices that characterize the Perticara mine (air, water, host-rock, minerals, and bitumen) were sampled and investigated employing a multi-analytical approach to define the distribution and origin of these hazardous elements. Water samples showed high Al, Fe, Pb, Mg, and Mn content but not radioactive elements. The bitumen sample showed a higher amount of ^{210}Po and ^{210}Pb (0.12 Bq/g and 0.11 Bq/g, respectively), compared to the host-rock and fibrous sericolite samples, but lower than fibrous epsomite crystals (^{210}Po 5.59 Bq/g; ^{210}Pb 5.93 Bq/g). A high ^{222}Rn concentration was also detected in the tunnels and it is likely the source of both ^{210}Po and ^{210}Pb, which are in radioactive equilibrium, especially in epsomite. This latter mineral, being capable of capturing ^{210}Po and ^{210}Pb, can be used as a helpful mineral indicator for the presence of radioactive elements in similar environmental conditions. Moreover, our results also highlight a slight anomaly in the ^{40}K and ^{226}Ra content of the host-rock, probably derived from the evaporitic sediments of the rock succession. The current risk for humans linked to the mine environment is minor since the activity of the mine ended several decades ago. However, the results of this study must be taken into serious consideration for any future development of this area (e.g., industrial

* Corresponding author at: Department of Pure and Applied Sciences, University of Urbino Carlo Bo, Urbino, Italy.
E-mail address: matteo.giordani@uniurb.it (M. Giordani).

https://doi.org/10.1016/j.scitotenv.2023.167498
Received 13 July 2023; Received in revised form 25 September 2023; Accepted 28 September 2023
Available online 29 September 2023

archaeology, farming, educational, scientific and touristic purposes), and represent the basis for the calculation of radiotoxicity and dose assessment, which is fundamental for the correct and safe management of the mining environment and neighbouring areas.

1. Introduction

Global concerns about fibrous minerals, potentially toxic elements, and radioactivity are steadily increasing due to their significant threats to human health and environmental quality. Concerning fibrous minerals, bio-persistent asbestos, zeolites and other silicates are toxic (or suspected to be) and thus deeply investigated to assess the effects on human health (Ballirano et al., 2018; Betti et al., 2022; Cangiotti et al., 2017; Gianfagna and Oberti, 2001; Giordani et al., 2016, 2022a; Gualtieri et al., 2021; Mattioli et al., 2018, 2022; Petriglieri et al., 2021). Nevertheless, a key role in fibrous minerals toxicity is not only linked to the size of the crystals but also to the chemical composition, encompassing the content of metals and other toxic elements, often attached as impurities on the surface of the fibres (Giordani et al., 2019, 2022b; Pacella et al., 2018). This is particularly true for the fibrous minerals highly soluble in water and biological fluids, which can release significant amounts of toxic elements.

Potentially toxic elements (PTEs) include both metals and metalloids, e.g., As, Cd, Hg, Pb, and Sb or micronutrients, e.g., Cr, Cu, Ni, Se, and Zn, that may become toxic when their concentrations exceed the tolerance limits (Han et al., 2021). The high levels of exposure of Pb, Fe and Mn cations increase the production of reactive oxygen species (ROS) in cells, which oxidizes biological proteins and may even cause cell death. In the case of Pb, the blood flow favours its distribution in the body and almost 95 % of lead is dumped in skeletal bones as insoluble phosphate (Khanam et al., 2020). The significant signs of Pb poisoning are mainly related to the central nervous system and the gastrointestinal tract, and its chronic exposure can result in several diseases (e.g., birth defects, brain damage, autism, allergies, paralysis, kidney damage) and may even cause death (Markowitz, 2000; Martin and Griswold, 2009). Regarding Fe and Mn, despite being essential metals for humans and playing an important role in many biological and physiological processes, exposure to high concentrations can have toxic effects. Excessive Mn may accumulate in the liver, kidney, and brain, resulting in harmful effects such as the development of Parkinson-like disorders (Tang et al., 2019). The main routes of exposure to PTEs include ingestion through indirect consumption of polluted foods, absorption through the consumption of water, direct skin contact with contaminated water and soil, and inhalation of dust (Antoniadis et al., 2017; Niede and Benbi, 2022).

Concerning radioactivity, about 70 radionuclides are present in the Earth's crust and are naturally found in air, water, soil, and building materials. Some have applications in many fields (e.g., agriculture, medicine, sterilization), but many others can have serious health implications (Ali et al., 2012; Paschoa and Steinhäusler, 2010). For example, ^{222}Rn and two of its short-lived progeny ^{218}Po and ^{214}Po (all alpha emitters) represent most of the risks for inhalation exposure (NRC, 1999; Vengosh et al., 2022). ^{222}Rn emission from a material depends on many factors, such as the concentration of U in the same matrix, its physical properties, and the climatic conditions (Keller and Schutz, 1988; Righi and Bruzzi, 2006). Exposure to high radon concentration can lead to lung cancer (US EPA, 2009) and its decay products deposited in the lung emit alpha particles, which damage the cells of the bronchial epithelium (Petermann et al., 2022). ^{210}Po is the penultimate daughter of the ^{238}U decay series and is an alpha-radioactive emitter with a half-life of 138.4 days before decaying to stable ^{206}Pb (e.g., Persson and Holm, 2011 and references therein). The natural radiation background of ^{210}Po in surface soils is in the range of 0.01–0.2 Bq/g depending on the bedrock, soil properties, depth of sampling, and climatic conditions (Carvalho et al., 2017; Meli et al., 2013). Similarly, ^{210}Pb is a progeny of ^{222}Rn and has one of the highest dose coefficient values, posing one of the higher risks to human health among radionuclides occurring in nature (Eckerman et al., 1999; WHO, 2017).

These issues coexist in the abandoned Perticara sulphur mine, where highly soluble epsomite crystals extensively grow with a fibrous habit and contain significant amounts of PTEs and radioactive elements (Giordani et al., 2022c). The Perticara mine is located on the Apennines chain in the Rimini province (Central Italy). It was developed in the Gessoso-Solfifera Formation (Messinian, Upper Miocene; Fig. 1), a rock succession mainly composed of gypsum, limestones, and marls (e.g., Rossi et al., 2021 and references therein; Roveri et al., 2003). The activity of the mine, developed on eight levels, started in the XVIII century and ceased in 1964. Nowadays, almost all the galleries are closed and very few air exchanges with the outside occur. Many galleries are flooded, while others are accessible only with self-protective equipment due to the absence of breathable air, poor in O_2 and rich in toxic compounds like CO_2 and H_2S (Belvederi et al., 2016).

Considering the possibility of re-opening the Perticara mine for educational, scientific, and touristic purposes, it is important to understand the distribution and possible source(s) of the potentially toxic and radioactive elements, to manage the mining environment and neighbouring areas correctly and safely. For these reasons, the different matrices inside the mine were sampled and investigated in this work. Several analytical techniques such as X-ray Powder Diffraction (XRPD), Environmental Scanning Electron Microscopy (ESEM-EDS), Inductively Coupled Plasma-Atomic Emission (ICP-AES), Inductively Coupled Plasma-Mass Spectrometry (ICP-MS), Atomic Absorption Spectrometry (AAS), Gamma Spectrometry, Alpha Spectrometry, Radon Monitor, and Alpha Track Detector (ATD) were combined and integrated to obtain a picture of information on the distribution and origin of these toxic and radioactive elements as complete as possible. These results could represent a fundamental reference for future studies that define the real risks for the environment and human health connected with mining activities.

2. Materials and methods

Representative samples of the different matrices that characterize the Perticara sulphur mine environment were collected and analysed: (I) natural fibrous epsomite crystals (labelled MP); (II) vein-filling fibrous gypsum (sericolite variety, MP_SER); (III) the host-rock where the mining tunnels were dug (MP_MAR); (IV) natural bitumen that emerges from the walls of the mine (MP_BIT); (V) dust deposited on the ground (MP_DUS); (VI) two different water discharges (WDO for water sample collected in “Discenderia Ovest”, and WDF for water sample collected in “Discenderia Fanante”, respectively). In Fig. 2, the sketch map of the mine galleries and the location of the collected samples are reported.

After collection, the samples were stored at about 20 °C, i.e., a temperature comparable to that of the mine, in airtight containers to prevent modifications or alteration, such as dehydration/hydration and the phase changes of the materials. Morphological observations and qualitative micro-chemical characterization were performed by ESEM with an energy-dispersive X-ray spectrometer (EDS), while mineralogical compositions were determined by XRPD. Detailed chemical compositions were obtained using ICP-AES, ICP-MS and AAS. For the ^{210}Po and ^{210}Pb determinations, an α-spectrometer was employed, and a high-purity germanium (HPGe) detector gamma spectrometer was used to measure the activity of gamma emitters. Moreover, active and passive measurements of the Radon content in the atmosphere of the mine were performed, as well as the direct measurements of gamma irradiation inside the mine galleries. The various analytical methods are described in detail in the Supplementary Material (S1).

3. Results

3.1. Morphology and micro-chemical characterization (ESEM-EDS)

The sample MP_SER occurs as fibrous gypsum (sericolite) filling a complex network of centimetric veins inside the host-rock. ESEM images show the presence of different layers up to 200 μm thick of highly fibrous gypsum in intergrowth with layers of massive-type gypsum (Fig. 3a). EDS analyses reveal a homogeneous composition (pure gypsum) for both varieties (20.75 wt% of CaO and 25.17 wt% of SO_3).

Epsomite (MP) extensively grows perpendicularly to the surface of walls and blocks inside the mine and is formed by very long fibrous crystals (up to 4 cm) with a small size in width (Fig. 3b). Morphometric details and chemical composition of epsomite fibres are reported in Giordani et al. (2022c).

3.2. Mineralogical composition

XRPD patterns of the investigated samples and their semi-quantitative mineralogical estimations are presented in Fig. 4 and Table 1, respectively. According to the relative pattern, the MP_SER sample consists of pure fibrous gypsum, as shown by the first-order d-spacing of 7.55 Å (2ϴ 11.72) accompanied by the minor peaks corresponding to 4.27 Å (2ϴ 20.81) and 3.79 Å (2ϴ 23.48) in the diffractogram. MP_DUS is a polycrystalline sample and is mainly composed of gypsum (7.56 Å, 4.27 Å and 3.79 Å), associated with moderate contents of dolomite (2.88 Å) and quartz (3.34 Å). Calcite (3.03 Å) and epsomite (4.21 Å, 5.33 Å and 2.66 Å) are present in minor amounts, while traces of phyllosilicates (mainly illite/mica group) are also detected (d-spacing value of 10 Å). MP sample pattern is consistent with the pure heptahydrate magnesium sulphate epsomite, showing the three strongest peaks corresponding to the (hkl) indices (020), (120) and (220). The highest peak intensity occurs at 2ϴ ~21°, corresponding to a d-spacing value of 4.21 Å. At 2.67 Å and 5.34 Å are positioned the two secondary reflections (0.25), while minor peaks correspond to d-spacing of 5.99 Å and 2.08 Å. The MP_MAR is a polycrystalline sample mainly composed of gypsum (7.56 Å, 4.27 Å and 3.79 Å), with a minor amount of quartz and dolomite (3.34 Å and 2.88 Å, respectively), while calcite (3.03 Å) and illite-mica (10 Å) are also present in traces. If we exclude the presence of epsomite, MP_MAR is compositionally very similar to the MP_DUS sample.

3.3. Chemical composition

The accurate chemical compositions of the sericolite (MP_SER), host-rock (MP_MAR), bitumen (MP_BIT), and two water (WDO and WDF) samples are reported in Table 2. The major chemical constituents of MP_SER are S and Ca (236,000 and 157,000 mg/kg, respectively) and are perfectly consistent with the gypsum phase (sericolite). A high amount of Si (1240 mg/kg) and significant contents of Sr (126 mg/kg) and Mg (65.8 mg/kg) were also detected. In addition, a minor amount (< 10 mg/kg) of Cu, Mn, Ti, Zn, Rb and Sn are present in the sericolite sample.

MP_MAR sample shows a more complex composition, reflecting the presence of different minerals in the host-rock, as previously observed by Giordani et al. (2022c). Accordingly, the contents of S and Ca (81,000 and 116,000 mg/kg, respectively) are very high and related to gypsum. However, the main element of the sample is Si (129,000 mg/kg), coupled with high contents of Al (25,200 mg/kg), Mg (22,600 mg/kg), Fe (17,600 mg/kg), K (11,300 mg/kg), Sr (3610 mg/kg) and Ti (1230 mg/kg), probably linked to the presence of silicates and carbonates (quartz, illite-mica, and dolomite). Moreover, significant contents of Mn (710 mg/kg), P (413 mg/kg), Ba (265 mg/kg), and minor amounts of Zn (82 mg/kg), Rb (71 mg/kg), Cr (66.2 mg/kg), Ni (44.8 mg/kg), Cu (29.6 mg/kg), Th (21 mg/kg) and As (16.1 mg/kg), were found in MP_MAR sample. Other elements are present in very low amounts (< 10 mg/kg; see Table 2).

The bitumen sample (MP_BIT) shows a high concentration of S and Ca (82,000 and 53,150 mg/kg, respectively), followed by Mg (6400 mg/kg), P (1,185 mg/kg), Fe (1115 mg/kg), Sr (493 mg/kg), Al (132.5 mg/kg), K (127 mg/kg) and Sn (126.5 mg/kg). Minor amounts of Mn (35.55 mg/kg) and Ti (23.9 mg/kg) were also detected, while other elements such as Ni, Pb, Ba, Cu, Cr_{tot} and As are <10 mg/kg.

Regarding the water composition, the two analysed samples (WDF

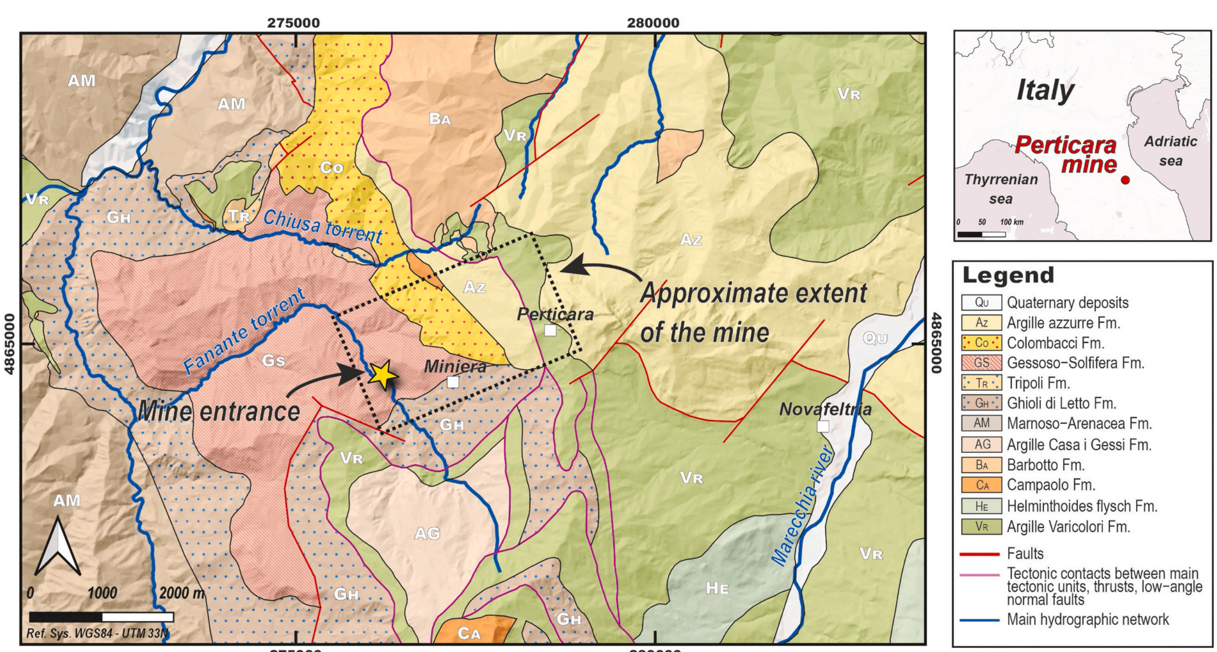

Fig. 1. Geological map of the Perticara sulphur mine (after Conti et al., 2020 and modified from Giordani et al., 2022c). The yellow star indicates the entrance of the mine; the black bolded rectangle indicates the approximate extent of the tunnel and galleries of the mine as inferred from Belvederi et al. (2016).

and WDO) show similar concentrations for most chemical components. They show high amounts of Mg (498–504 mg/L, respectively) and Mn (>1880 μg/L). However, significant differences can be highlighted between WDF and WDO samples, respectively, in the concentration of Al (479 vs. 49 μg/L), As (7.1 vs. 0.9 μg/L), Co (1.6 vs. 0.1 μg/L), Cr_{tot} (23.8 vs. 1.3 μg/L), Fe (32,906 vs. 117 μg/L), Ni (11.4 vs. 4.1 μg/L), Pb (17.5 vs. 0.7 μg/L), Cu (14.3 vs. 3.3 μg/L), and Ti (11.7 vs. <1 μg/L).

3.4. ^{210}Po and ^{210}Pb concentration

The concentration of ^{210}Po and the relative standard deviation (SD) in the investigated solid samples are shown in Table 3. The mean concentration of ^{210}Po (Bq/g) obtained by six replicates presents the following trend: MP_SER (0.039 ± 0.01) < MP_MAR (0.088 ± 0.02) < MP_BIT (0.12 ± 0.015). However, all samples present a significantly smaller amount of polonium than the epsomite fibres (5.59 Bq/g; Giordani et al., 2022c). Table 3 also shows ^{210}Pb mean activity concentration (Bq/g) for MP_BIT and MP samples, obtained with six replicates and the relative standard deviation (SD). In both samples the ^{210}Pb results in secular radioactive equilibrium with ^{210}Po. In water samples (WDF and WDO), only ^{210}Po was determined. The activity was 0.012 ± 0.001 and 0.013 ± 0.001 (Bq/L), respectively.

3.5. Gamma spectrometry

Host-rock (MP_MAR), epsomite (MP), and dust samples (MP_DUS) were investigated employing high-purity germanium (HPGe) radiation detectors, and the results are resumed in Table 4. The rock sample (MP_MAR) shows a low amount of radioactive elements. The average concentrations of ^{40}K and ^{238}U are 0.38 Bq/g and 0.08 Bq/g, respectively. ^{226}Ra reaches a value of 0.052 Bq/g; both ^{232}Th and ^{228}Ra show a value of 0.022 Bq/g, while ^{228}Th has a value of 0.019 Bq/g. ^{230}Th, ^{210}Pb, and ^{235}U are below the minimum detectable activity (MDA). The dust sample (MP_DUS) shows a slight variability in the radioactive elements content, but the detected amount is generally low. ^{40}K content (average) is 0.295 Bq/g, while that of ^{238}U is 0.061 Bq/g, ^{226}Ra is 0.029 Bq/g, and ^{228}Th is 0.017 Bq/g. The concentration of ^{232}Th is the same as ^{228}Ra, i.e., 0.018 Bq/g. Similarly to the previous sample, ^{230}Th, ^{210}Pb, and ^{235}U are below the MDA. The composition of the epsomite (MP) is significantly different: the radioactive element content is always below the MDA, except for ^{210}Pb, which is very high, with an average value of 3.7 Bq/g.

3.6. Radon concentration and alpha trace detector

The ^{222}Rn measurement results, collected according to the pathway

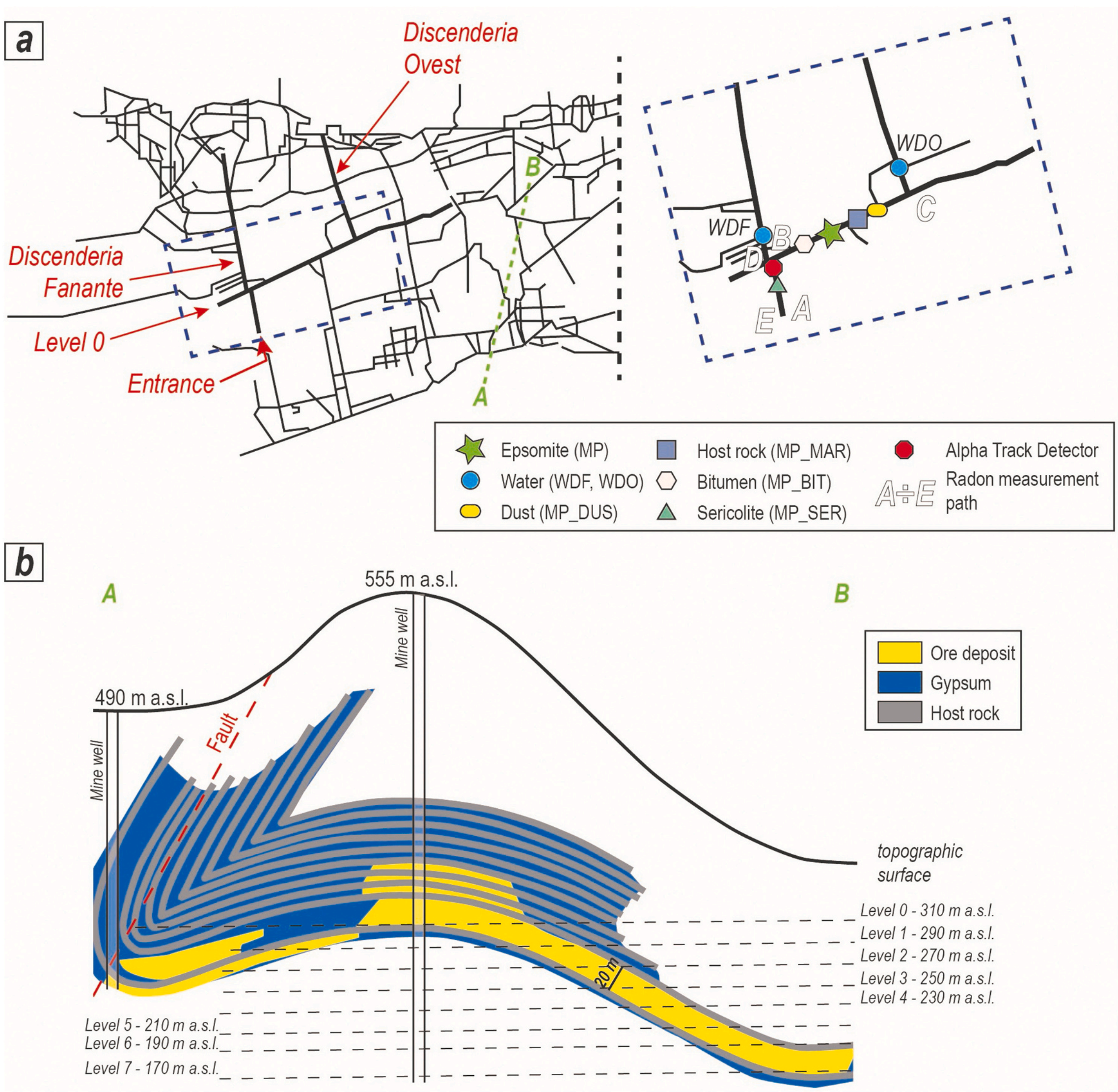

Fig. 2. (a) Sketch map of Perticara sulphur mine galleries with the collected samples' location (inset). (b) Geologic cross section of the Perticara area. Modified from Rinaldi, 1987.

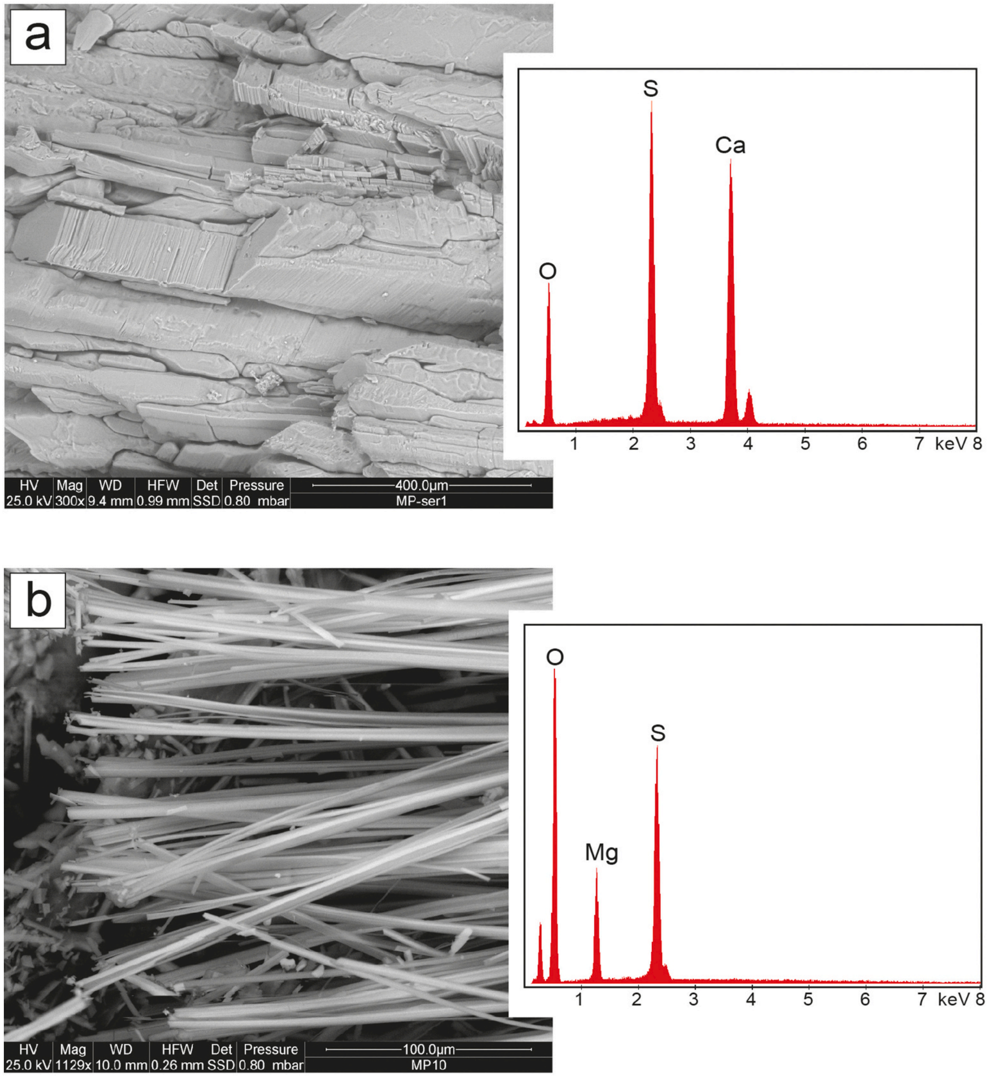

Fig. 3. a) ESEM microphotograph of sericolite sample (MP_SER), where different types of gypsum can be observed, and related EDS spectra. b) ESEM microphotograph of the fibrous epsomite sample (MP) and related EDS spectra.

A-B-C-D-E, are shown in Fig. 5. Immediately after entering the mine, the level of ^{222}Rn present in the air constantly increased until it exceeded the 800 Bq/m^3 value. During the stay in the areas furthest from the entrance, the recorded value always remained around 800 Bq/m^3, with some points exceeding this value and reaching the maximum value of 972 Bq/m^3. On the way out of the mine, the value rapidly dropped, with a rate similar to that occurred during entry. It should be noted that the reported value corresponds to an average measurement collected in a time of 10 min of measurement. Another exciting result comes from the passive monitoring of ^{222}Rn. Due to the prohibitive condition of the mine (absence of breathable air and its variation related to external atmospheric pressure), it was possible to recover only one of the passive dosimeters installed inside the mine. The recovered alpha trace detector was positioned inside the tunnels in the closest position to the entrance of the Perticara mine (Fig. 2). The average value of the concentration of ^{222}Rn, relating to about six months of measurements, reveals the value of 2200 ± 300 Bq/m^3.

3.7. Gamma irradiation

A diagram of the measurement of gamma irradiation in terms of environmental dose equivalent H*(10) trend is shown in Fig. 5. The collected data inside the mine showed slightly higher values than the environmental background outside (evaluable at 30–60 nSv/h), settling on average at values of 60–80 nSv/h with peaks up to 120 nSv/h.

4. Discussion

The analyses of WDO and WDF water samples reveal PTEs concentrations generally lower than the limits imposed by the Italian legislation for domestic and/or industrial usage (Law Decree 152/2006 3 April 2006, and subsequent amendments), with the exceptions of Mn, Al, Fe and Pb. Regarding Mn, it is 37 times the threshold limit (50 µg/L), which could be linked to the natural abundance of Mn oxides in the area (Ruggieri, 1970). The concentration values of Al, Fe, and Pb also exceed the threshold values set at 200, 200, and 10 µg/L, respectively (Table 2). Despite being a parameter not regulated by law, the amount of Mg is much higher than those measured in other surrounding spring waters in a similar geological context, which usually have Mg $<$117 mg/L (D'Angeli and De Waele, 2016). It cannot be excluded that a contribution to these relevant concentrations may derive from the weathering of the abandoned material and railway tracks. Strong enrichments, primarily in Na^+ and SO_4^{2-} and secondly in Ca^{2+} and Mg^{2+}, have already been reported for the Perticara mine (Peruzzi et al., 2016) and have been linked to interaction processes between circulating waters and the host rock (Roveri et al., 2003). The concentration of ^{210}Po in water samples

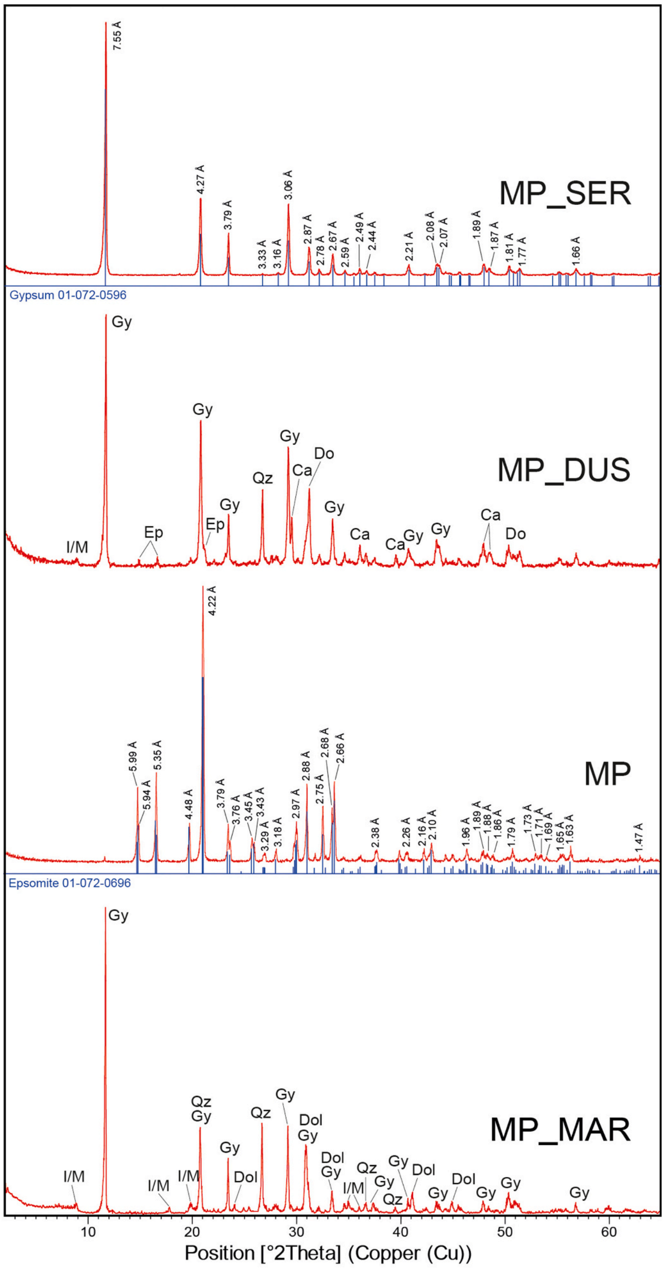

Fig. 4. XRPD patterns of the investigated samples. MP_SER = pure fibrous gypsum (sericolite); MP_DUS = dust deposited on the ground; MP = pure epsomite crystals (from Giordani et al., 2022c); MP_MAR = host-rock (from Giordani et al., 2022c).

Table 1
Semi-quantitative mineralogical composition of the investigated samples determined by XRPD using CuK radiation. MP_SER = pure fibrous gypsum (sericolite); MP_DUS = dust deposited on the ground; MP = pure epsomite crystals (from Giordani et al., 2022c); MP_MAR = marly host-rock (from Giordani et al., 2022c). +++ ≥ 60 %; ++ = 60 %–30 %; + = 30 %–5 %; TR (traces) ≤ 5 %.

	MP_SER	MP_DUS	MP	MP_MAR
Epsomite	–	+	+++	–
Gypsum	+++	+++	–	+++
Calcite	–	+	–	tr
Dolomite	–	++	–	++
Quartz	–	++	–	++
Illite/Mica	–	tr	–	tr

from the Perticara mine (0.012 and 0.013 Bq/L, respectively) are comparable with the values reported in the literature for groundwater (Persson and Holm, 2011) and perfectly fit in the range of mineral waters sampled in Italy (0.0004–0.021 Bq/L; Desideri et al., 2007). Typically, ^{210}Po has a very low solubility (Desideri et al., 2007; Seiler et al., 2011) and, in the Perticara mine, the concentrations are much lower than the limit value of 0.1 Bq/L for drinking water (Linkevičius, 2013; WHO, 2011).

Moving to solid samples, sericolite (MP_SER) and host rock (MP_MAR) show low concentrations of ^{210}Po (0.039 ± 0.01 Bq/g and 0.088 ± 0.02 Bq/g, respectively). These amounts are comparable with a typical radiation background for surface soils (0.01–0.2 Bq/g; Carvalho et al., 2017). Concerning the host-rock sample, the concentration of ^{210}Po is also similar to the values of the original ^{238}U (0.080 Bq/g) and intermediate ^{226}Ra (0.052 Bq/g), indicating secular equilibrium of the radionuclides. The concentration of ^{210}Po increases in the bitumen sample (MP_BIT; 0.12 ± 0.02 Bq/g), in equilibrium with the original ^{210}Pb (0.11 ± 0.02 Bq/g) content. This means it is polonium-supported, which exclusively results from the on-site decay of ^{210}Pb and not from other external sources. The concentrations of ^{210}Po and ^{210}Pb reach the maximum values in the epsomite sample (5.59 and 5.93 Bq/g, respectively). These values are also confirmed by ^{210}Pb gamma spectrometry data (3.7 Bq/g), while ^{238}U and ^{226}Ra were not detected. Although epsomite shows the highest concentration of ^{210}Po and ^{210}Pb, natural bitumen is also interesting, reaching a value one order of magnitude higher than in the other investigated matrices. Contrarily to ^{238}U and ^{232}Th, some of their related decay products are slightly soluble and can be mobilized in the liquid phases (Smith, 1992). Then, the concentration of ^{210}Po and ^{210}Pb in the bitumen could be linked to the ^{238}U and ^{232}Th present in the host-rock and to the mobility of the related decay products in hydrocarbons and water, as suggested by Smith (1992). In addition, the major carrier phases for Po are related to biological processes rather than inorganic particles (Wei and Murray, 1994). Evidence of ^{210}Po remobilization from sediment under both anoxic and hypoxic conditions was observed in the seawater column by Jones et al. (2015). Several authors (Lehto et al., 1999; Persson and Holm, 2011; Vaaramaa et al., 2003) hypothesized that redox-sensitive metals such as Fe and Mn, coupled with the degradation of organic matter, are the fundamental mechanisms for ^{210}Po remobilization. In the Perticara mine, high concentrations of Fe, Mn and organic matter are present, and despite the different conditions (continental environment), similar processes may occur.

The content of ^{40}K in the investigated host-rock sample MP_MAR (0.38 Bq/g) is higher than the literature (Table S2, Supplementary Material). It is important to note that our host-rock sample is mainly composed of gypsum coupled with a low amount of carbonate and very low clay fraction content. Clay minerals are generally the principal source of natural gamma rays due to their ability to fix K, U and Th. Uranium is strictly related to the organic matter content, enrichment processes (authigenic uranium), and then to the detrital grains input, while ^{40}K and ^{232}Th are associated with the clastic fraction (Manzi et al., 2007; Sampalmieri et al., 2010; Sierro et al., 2000). Considering ^{226}Ra, MP_MAR shows an activity of 0.052 Bq/g, which is significantly higher than the literature data for gypsum. In the case of ^{232}Th, the value of 0.022 Bq/g perfectly fits in the range for all the sedimentary rocks considered as reference (Table S2). Therefore, the slight anomaly on ^{40}K and ^{226}Ra radioisotopes observed in the investigated host-rock could be related to a higher presence of K and U (and related decay series) in the original sediments and rock formations.

In nature, the exhalation of ^{222}Rn into the atmosphere is the primary source of ^{210}Pb, which decays in ^{210}Po through ^{210}Bi (Jones et al., 2015 and references therein). Although ^{210}Po is produced from ^{210}Pb decay within the atmosphere, this activity represents a relatively small fraction of the ^{210}Pb activity because of the short atmospheric residence time of ^{210}Pb-containing aerosols (Harada et al., 1989; Kim et al., 2005). However, the confined atmosphere makes the Perticara mine a very

Table 2
Major and minor element concentrations in investigated samples. MP from Giordani et al. (2022c). The symbol < means below the detection limit.

Element	MP_SER mg/kg	MP_MAR mg/kg	MP_BIT mg/kg	MP mg/kg	WDF mg/L	WDO mg/L
Al	<0.1	25,200	132.5	100	0.476	0.049
Sb	<5	<5	<5	<5	0.0009	0.0002
As	<1	16.1	1.00	3	0.0071	0.0009
Ba	<0.5	265	3.15	<0.5	0.0108	0.0083
Cd	<0.5	0.5	<0.5	<0.5	<0.0001	<0.0001
Ca	157,000	116,000	53,150	1030	417	421
Co	<0.5	9.9	0.60	0.5	0.0016	0.0001
Cr (tot)	<1	66.2	2.5	<1	0.0238	0.0013
Fe	<5	17,600	1115	94	32.906	0.117
P	<0.5	413	1185	7.2	0.72	0.230
Mg	65.8	22,600	6400	77,000	504	498
Mn	7.4	710	35.55	36	2.073	1.881
Ni	<0.5	44.8	6.85	11	0.0114	0.0041
Pb	<0.5	9.8	5.05	<0.5	0.0175	0.0007
K	<0.5	11,300	127	120	31.0	32.1
Cu	8.3	29.6	2.5	<1	0.0141	0.0033
Si	1240	129,000	<10	204	19.1	15.3
Sn	3.44	7.7	126.5	<0.2	<0.0005	<0.0005
Sr	126	3610	493	7.2	9.587	9.069
Tl	<0.1	<0.1	<0.1	<0.1	<0.0001	<0.0001
Te	<0.5	<0.5	<0.5	<0.5	<0.001	<0.001
Ti	7	1230	23.9	5.3	0.0117	<0.001
Th	<5	21	<5	<5	<0.001	<0.001
Zn	5.93	82	<0.5	18.4	0.112	0.024
S	236,000	81,000	82,000	127,000	4760	4050
Ce	<10	<10	<10	<10	0.002	<0.001
La	<1	5	<1	<1	0.001	<0.001
Rb	5	71	<1	<1	0.018	0.017
U	<1	<1	<1	<1	<0.001	<0.001
Hg	<0.0005	0.027	0.185	<0.0005	<0.0001	<0.0001

Table 3
^{210}Po and ^{210}Pb mean concentration and standard deviation (SD) in the analysed samples. The concentration of ^{210}Po in the MP sample (from Giordani et al., 2022c) is also reported for comparison.

Sample	^{210}Po (Bq/g)	^{210}Pb (Bq/g)
MP_SER	0.039 ± 0.01 *(SD 0.005)*	–
MP_MAR	0.088 ± 0.02 *(SD 0.005)*	–
MP_BIT	0.12 ± 0.02 *(SD 0.015)*	0.11 ± 0.02 *(SD 0.032)*
MP	5.59 ± 0.84 *(SD 1.11)*	5.93 ± 1.19 *(SD 0.54)*
	^{210}Po (Bq/L)	^{210}Pb (Bq/L)
WDF	0.013 ± 0.001 *(SD 0.003)*	–
WDO	0.012 ± 0.001 *(SD 0.003)*	–

particular environment with a very low content of oxygen and high amounts of other gases (e.g., CO_2 and H_2S) (Belvederi et al., 2016). Similarly, the high ^{222}Rn concentration in the galleries (800 Bq/m^3 from direct measurement and 2200 ± 300 Bq/m^3 from 6 months average) is likely related to the confined atmosphere, even with different values during time. This variability is probably linked to barometric pressure and ventilation and can follow the dynamics of the other gases in the

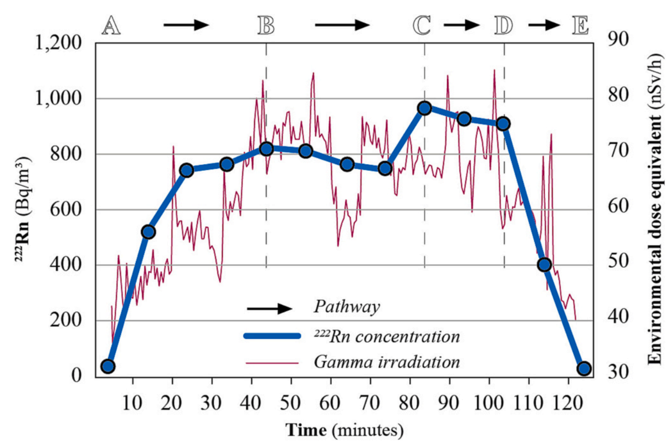

Fig. 5. ^{222}Rn concentration values and gamma irradiation trend detected in the galleries of Perticara sulphur mine. The data collection was performed during the pathway inside the galleries (sequence A-B-C-D-E as reported in Fig. 2). For the gamma irradiation graph, each reported point corresponds to the average of 30 measurements.

Table 4
The average concentration of radiogenic elements, in Bq/g, measured by HPGe radiation detectors on host-rock (MP_MAR), dust samples (MP_DUS), and epsomite (MP). The minimum detectable activity (MDA) for each sample and element is also reported. *Evaluation based on gamma emission of related short-life decay elements.

Sample	MP_MAR	MDA	MP_DUS	MDA	MP	MDA
^{40}K	0.38 ± 0.050	0.029	0.295 ± 0.040	0.025	<	0.13
^{238}U (from ^{234}Th)*	0.080 ± 0.027	0.051	0.061 ± 0.022	0.041	<	0.97
^{230}Th	<	0.51	<	0.4	<	4.6
^{226}Ra (from ^{214}Pb)	0.052 ± 0.007	0.0038	0.029 ± 0.005	0.0048	<	0.14
^{210}Pb	<	0.083	<	0.074	3.70 ± 0.90	1.3
^{232}Th (from ^{228}Ac)*	0.022 ± 0.007	0.0086	0.018 ± 0.007	0.0059	<	0.31
^{228}Ra (from ^{228}Ac)*	0.022 ± 0.007	0.0086	0.018 ± 0.007	0.0059	<	0.31
^{228}Th (from ^{212}Pb)*	0.019 ± 0.004	0.0035	0.017 ± 0.003	0.0035	<	0.088
^{235}U	<	0.012	<	0.015	<	0.32

network galleries (Belvederi et al., 2016; Sahu et al., 2016). Here, ^{222}Rn tends to accumulate since the activities of the mine ceased, and higher concentration in the furthest galleries is also expected. WHO recommends a radon concentration threshold in buildings of 100 Bq/m^3 (WHO, 2009), and the derived air concentration (DAC) limit for radon and its daughters in mine workplaces is 1000 Bq/m^3 (IAEA, 2003; ICRP, 1993). Then, the radon concentration in the mine is more than significant. Moreover, the decay daughters of ^{222}Rn probably remain in the galleries, resulting in the high amounts of ^{210}Pb and ^{210}Po detected in the investigated samples, mainly in epsomite (MP). In groundwater, it has been observed that the occurrence of ^{210}Pb is directly associated with ^{222}Rn (Seiler et al., 2011; Vengosh et al., 2022). Similar ^{210}Pb and ^{210}Po anomalies may be due to reducing conditions, sulphate reduction, manganese oxide dissolution and high pH in the water-air interface environment. In particular, ^{210}Po can be strongly related to sulphur recycling and the dissolution and reprecipitation of sulphur minerals (Seiler et al., 2011; WHO, 1999). The lowest concentration of ^{210}Po in MP_SER (another secondary phase) could be explained by the proximity to the mine entrance, where ^{222}Rn was more easily released to the external environment. Alternatively, sericolite could be formed before the mine closure, while epsomite (MP) formed after.

Currently, considering that neither miners (or workers in general) nor tourists have access to the galleries, there is no exposition and the risk to human health related to the Perticara mine should be considered negligible. However, the real possibility of re-opening this mining site for educational, scientific and touristic purposes makes it essential to have an accurate knowledge of the related environmental conditions and, particularly, the potential risk factors (e.g., PTEs and radioactive elements). Additionally, it is also of relevant importance to shed light on comprehensive PTEs of farmland crops in the vicinity of abandoned sulphur mines and associated smelting areas, as well as possible aquifer-river hydrogeological connections, to evaluate the health risks for humans in consuming such crops. Moreover, it should be understood whether similar conditions, particularly the concentration of ^{222}Rn, ^{210}Po, ^{210}Pb and PTEs can also be present in other mines in comparable geological environments. In any case, it is important to underline that, in the case of radioactive elements, high activity concentration does not necessarily imply a higher effective dose, which is a derived quantity involving a well-known relationship between measured physical quantities, environmental conditions and biological effects.

5. Conclusions

In this work, a comprehensive analytical approach was applied to different geological matrices of the abandoned Perticara sulphur mine to know the distribution and origin of toxic and radioactive elements in this peculiar environment. The main results of the study raise various points of concern.

Epsomite crystals are the only samples that showed high concentrations of ^{210}Po and ^{210}Pb, while ^{238}U and ^{226}Ra were not detected in the same minerals. Bitumen also presented relevant ^{210}Po activities in equilibrium with ^{210}Pb. The rest of the solid samples (sericolite and host-rock) showed, in fact, ^{210}Po content typical of surface soils, with the value of other radioactive elements (^{238}U and ^{226}Ra) indicative of a secular radioactive equilibrium of the radionuclides. The slight anomaly on ^{40}K and ^{226}Ra contents observed in the host-rock can be likely related to a higher presence of K and U (and related decay series) in the original sediments and rock formations. Also, the ^{210}Po content is consistent with groundwater values in the water discharges inside the mine. On the contrary, these waters revealed high concentrations of Al, Fe, Pb, Mg and, particularly, Mn. As the surficial waters are used for human, agricultural, and pastoral activities, these anomalies and possible aquifer-river hydrogeological connections should be further investigated. The confined atmosphere of the mine, with the high ^{222}Rn concentration, is likely the source of the high level of ^{210}Po and ^{210}Pb, in radioactive equilibrium, detected in epsomite fibres. Thus, the ^{222}Rn-rich, anoxic, and hypoxic atmosphere, coupled with the abundance of Mn, Fe, and organic matter in the mine, could play a key role in the ^{210}Po remobilization.

This work highlighted that natural epsomite, which is a very common mineral phase in mines, caves, and underground environments, is able to capture ^{210}Po and ^{210}Pb. For this reason, it can be used as a helpful mineral indicator for the presence of radioactive elements in similar environmental conditions, also helping to ensure safe management. No target is currently exposed to these hazardous elements in the Perticara sulphur mine, as it is abandoned. However, there is a real possibility of re-opening this site for educational, scientific and touristic purposes, as happened for many other mines in recent years (e.g., Price, 2021; Sorcaru, 2021). Since high concentration doesn't mean it may be harmful, the results of our study represent the basis for the calculation of radiotoxicity and dose assessment in the real scenario connected to visiting the mine, which is fundamental for the correct and safe management of the mining environment and neighbouring areas. These results indicate that in areas with a long history of mining, despite decommissioning, environmental hazards and human health risks may still emerge in terms of radioactivity and PTEs. The current awareness of environmental contamination caused by local mines is often insufficient and some risks due to exposure to PTEs and radioactive elements still need to be addressed in some areas.

Funding

This research was conducted within the research project “Fibres, A Multidisciplinary Mineralogical, Crystal-Chemical and Biological Project to Amend the Paradigm of Toxicity and Cancerogenicity of Mineral Fibres” (Code PRIN20173X8WA4). This work was also funded under the framework of the 2022 research programs of the Department of Pure and Applied Sciences of the Università di Urbino Carlo Bo (project “New asbestiform fibers: mineralogical and physical-chemical characterization”, responsible M. Mattioli).

CRediT authorship contribution statement

Matteo Giordani: Conceptualization, Investigation, Visualization, Project administration, Data curation, Formal analysis, Supervision, Writing – original draft. **Marco Taussi:** Data curation, Investigation, Visualization, Writing – review & editing. **Maria Assunta Meli:** Data curation, Formal analysis, Writing – review & editing. **Carla Roselli:** Data curation, Formal analysis, Writing – review & editing. **Giacomo Zambelli:** Formal analysis, Writing – review & editing. **Ivan Fagiolino:** Formal analysis. **Michele Mattioli:** Data curation, Investigation, Formal analysis, Funding acquisition, Writing – review & editing.

Declaration of competing interest

The authors declare no competing interests.

Data availability

Data will be made available on request.

Acknowledgment

The authors are grateful to: Laura Valentini (University of Urbino Carlo Bo) for her kind help in collecting ESEM images; Fabio Peruzzi (Federazione Speleologica Emilia-Romagna), Michele Betti (University of Urbino Carlo Bo and Gruppo Speleologico Urbino), Sara Camilletti (Gruppo Speleologico Montelago and Centro di Speleologia Montelago), Enrico Maria Sacchi, Ivan Munari, Massimo Vagnini and Thomas Sperandio (Gruppo Speleologico Urbino), for their essential support and collaboration during sampling phases. “Museo Sulphur” of Perticara (Novafeltria, RN, Italy) is also acknowledged for making its facilities available and for the kind collaboration. Three anonymous reviewers and the associate editor (Daniel S. Alessi) are sincerely thanked for their insightful and thoughtful comments.

Appendix A. Supplementary data

Supplementary data to this article can be found online at https://doi.org/10.1016/j.scitotenv.2023.167498.

References

Ali, M., Qureshi, A.A., Waheed, A., Baloch, M.A., Qayyum, H., Tufail, M., Khan, H.A., 2012. Assessment of radiological Hazard of NORM in Margalla Hills limestone, Pakistan. Environ. Monit. Assess. 184 (8), 4623–4634. https://doi.org/10.1007/s10661-011-2290-5. Springer.

Antoniadis, V., Levizou, E., Shaheen, S.M., Sik Ok, Y., Sebastian, A., Baum, C., Prasad, M. N.V., Wenzel, W.W., Rinklebe, L., 2017. Trace elements in the soil-plant interface: phytoavailability, translocation, and phytoremediation – a review. Earth Sci. Rev. 171, 621–645. https://doi.org/10.1016/j.earscirev.2017.06.005.

Ballirano, P., Pacella, A., Bloise, A., Giordani, M., Mattioli, M., 2018. Thermal stability of woolly erionite-K and considerations about the heat-induced behaviour of the erionite group. Minerals 8 (1), 28. https://doi.org/10.3390/min8010028.

Belvederi, G., Ercolani, M., Garberi, M.L., Gonnella, S., Leandri, O., Peruzzi, F., Rossi, G., Sansavini, B., 2016. Miniera di Perticara: la complessa riesplorazione. In: GESSI E SOLFI DELLA ROMAGNA ORIENTALE, 31. Memorie dell'Istituto Italiano di Speleologia s. II, pp. 279–346.

Betti, M., Nasoni, M.G., Luchetti, F., Giordani, M., Mattioli, M., 2022. Potential toxicity of natural fibrous zeolites: in vitro study using Jurkat and HT22 cell lines. Minerals 12 (8), 988. https://doi.org/10.3390/min12080988.

Cangiotti, M., Battistelli, M., Salucci, S., Falcieri, E., Mattioli, M., Giordani, M., Ottaviani, M.F., 2017. Electron paramagnetic resonance and transmission electron microscopy study of the interactions between asbestiform zeolite fibers and model membranes. J. Toxicol. Environ. Health – A: Curr. Issues 80 (3), 171–187. https://doi.org/10.1080/15287394.2016.1275901.

Carvalho, F., Fernandes, S., Fesenko, S., Holm, E., Howard, B., Martin, P., Phaneuf, M., Porcelli, D., Pröhl, G., Twining, J., 2017. The environmental behaviour of polonium. Int. Atomic Energy Agency 484.

Conti, P., Cornamusini, G., Carmignani, L., 2020. An outline of the geology of the northern Apennines (Italy), with geological map at 1:250,000 scale. Italian J. Geosci. 139 (2), 149–194. https://doi.org/10.3301/IJG.2019.25.

D'Angeli, I.M., De Waele, J., 2016. Analisi chimico-fisiche delle acque campionate nei gessi messiniani nelle province di Forlì-Cesena e Rimini. In: GESSI E SOLFI DELLA ROMAGNA ORIENTALE. Memorie dell'Istituto Italiano di Speleologia, s. II, 31, 2016, pp. 169–180.

Desideri, D., Meli, M.A., Feduzi, L., Roselli, C., Rongoni, A., Saetta, D., 2007. ^{238}U, ^{234}U, ^{226}Ra, ^{210}Po concentrations of bottled mineral waters in Italy and their dose contribution. J. Environ. Radioact. 94, 86–97. https://doi.org/10.1016/j.jenvrad.2007.01.005.

Eckerman, K.F.L., Leggett, R.W., Nelson, C.B., Puskin, J.S., Richardson, A.C.B., 1999. Cancer Risk Coefficients for Environmental Exposure to Radionuclides. EPA 402-R-99-001. Oak Ridge National Laboratory, Oak Ridge, Tennessee. https://www.nrc.gov/docs/ML1801/ML18019B163.pdf.

Gianfagna, A., Oberti, R., 2001. Fluoro-edenite from Biancavilla (Catania, Sicily, Italy): crystal chemistry of a new amphibole end-member. Am. Mineral. 86 (11−12), 1489–1493. https://doi.org/10.1180/0026461036760160.

Giordani, M., Mattioli, M., Dogan, M., Dogan, A.U., 2016. Potential carcinogenic erionite from Lessini Mounts, NE Italy: morphological, mineralogical and chemical characterization. J. Toxicol. Environ. Health 79 (18), 808–824. https://doi.org/10.1080/15287394.2016.1182453.

Giordani, M., Cametti, G., Di Lorenzo, F., Churakov, S.V., 2019. Real-time observation of fibrous zeolites reactivity in contact with simulated lung fluids (SLFs) obtained by atomic force microscope (AFM). Minerals 9 (2), 83. https://doi.org/10.3390/min9020083.

Giordani, M., Ballirano, P., Pacella, A., Meli, M.A., Roselli, C., Di Lorenzo, F., Fagiolino, I., Mattioli, M., 2022a. Another potentially hazardous zeolite from northern Italy: fibrous mordenite. Minerals 12 (5), 627. https://doi.org/10.3390/min12050627.

Giordani, M., Mattioli, M., Cangiotti, M., Fattori, A., Ottaviani, M.F., Betti, M., Ballirano, P., Pacella, A., Di Giuseppe, D., Scognamiglio, V., Hanuskova, M., 2022b. Characterisation of potentially toxic natural fibrous zeolites by means of electron paramagnetic resonance spectroscopy and morphological-mineralogical studies. Chemosphere 291, 133067. https://doi.org/10.1016/j.chemosphere.2021.133067.

Giordani, M., Meli, M.A., Roselli, C., Betti, M., Peruzzi, F., Taussi, M., Valentini, L., Fagiolino, I., Mattioli, M., 2022c. Could soluble minerals be hazardous to human health? Evidence from fibrous epsomite. Environ. Res. 206 https://doi.org/10.1016/j.envres.2021.112579.

Gualtieri, A.F., Zoboli, A., Filaferro, M., Benassi, M., Scarfì, S., Mirata, S., Avallone, R., Vitale, G., Bailey, M., Harper, M., Di Giuseppe, D., 2021. In vitro toxicity of fibrous glaucophane. Toxicology 454, 152743. https://doi.org/10.1016/j.tox.2021.152743.

Han, B., Weatherley, A.J., Mumford, K., Bolan, N., He, J.Z., Stevens, G.W., Chen, D.L., 2021. Modification of naturally abundant resources for remediation of potentially toxic elements: a review. J. Hazard. Mater. 421, 126775. https://doi.org/10.1016/j.jhazmat.2021.126755.

Harada, K., Burnett, W.C., LaRock, P.A., Cowart, J.B., 1989. Polonium in Florida groundwater and its possible relationship to the sulfur cycle and bacteria. Geochim. Cosmochim. Acta 53, 143–150. https://doi.org/10.1016/0016-7037(89)90281-0.

IAEA, 2003. Radiation Protection Against Radon in Workplaces Other Than Mines, vol 33. International Atomic Energy Agency (IAEA), Vienna.

ICRP, 1993. Protection against radon at home and at work. In: International Commission on Radiological Protection. ICRP Publication No. 65, vol 23, p. 2.

Jones, P., Maiti, K., McManus, J., 2015. Lead-210 and Polonium-210 disequilibria in the northern Gulf of Mexico hypoxic zone. Mar. Chem. 169, 1–15. https://doi.org/10.1016/j.marchem.2014.12.007.

Keller, G., Schutz, M., 1988. Radon exhalation from the soil. Radiat. Prot. Dosimetry 24 (1–4), 43–46. https://doi.org/10.1093/oxfordjournals.rpd.a080238.

Khanam, R., Kumar, A., Nayak, A.K., Shahid, M., Tripathi, R., Vijayakumar, S., Bhaduri, D., Kumar, U., Mohanty, S., Panneerselvam, P., Chatterjee, D., 2020. Metal (loid)s (As, Hg, Se, Pb and Cd) in paddy soil: bioavailability and potential risk to human health. Sci. Total Environ. 699, 134330. ISSN 0048-9697. https://doi.org/10.1016/j.scitotenv.2019.134330.

Kim, G., Hong, Y.L., Jang, J., Lee, I., Hwang, D.W., Yang, H.S., 2005. Evidence for anthropogenic ^{210}Po in the urban atmosphere of Seoul, Korea. Environ. Sci. Technol. 39 (6), 1519–1522. https://doi.org/10.1021/es049023u.

Lehto, J., Kelokaski, P., Vaaramaa, K., Jaakkola, T., 1999. Soluble and particle-bound Po-210 and Pb-210 in groundwaters. Radiochim. Acta 85, 149–155. https://doi.org/10.1524/ract.1999.85.34.149.

Linkevičius, L., 2013. Council directive 2013/51/EURATOM of 22 October 2013 laying down requirements for the protection of the health of the general public with regards to radioactive substances in water intended for human consumption. Off. J. Eur. Union 296, 12–16. https://doi.org/10.1016/j.scitotenv.2016.05.044.

Manzi, V., Roveri, M., Gennari, R., Bertini, A., Biffi, U., Giunta, S., Iaccarino, S.M., Lanci, L., Lugli, S., Negri, A., Riva, A., 2007. The deep-water counterpart of the Messinian Lower Evaporites in the Apennine foredeep: the Fanantello section (Northern Apennines, Italy). Palaeogeogr. Palaeoclimatol. Palaeoecol. 251 (3–4), 470–499. https://doi.org/10.1016/j.palaeo.2007.04.012.

Markowitz, M., 2000. Lead poisoning: a disease for the next millennium. Curr. Probl. Pediatr. 30 (3), 62–70. https://doi.org/10.1067/mps.2000.104053.

Martin, S., Griswold, W., 2009. Human health effects of heavy metals. In: Environmental Science and Technology Briefs for Citizens, 15, p. 5.

Mattioli, M., Giordani, M., Arcangeli, P., Valentini, L., Boscardin, M., Pacella, A., Ballirano, P., 2018. Prismatic to asbestiform offretite from northern Italy: occurrence, morphology and crystal-chemistry of a new potentially hazardous zeolite. Minerals 8 (2), 69. https://doi.org/10.3390/min8020069.

Mattioli, M., Ballirano, P., Pacella, A., Cangiotti, M., Di Lorenzo, F., Valentini, L., Meli, M.A., Roselli, C., Fagiolino, I., Giordani, M., 2022. Fibrous ferrierite from northern Italy: mineralogical characterization, surface properties, and assessment of potential toxicity. Minerals 12 (5), 626. https://doi.org/10.3390/min12050626.

Meli, M.A., Cantaluppi, C., Desideri, D., Benedetti, C., Feduzi, L., Ceccotto, F., Fasson, A., 2013. Radioactivity measurements and dosimetric evaluation in meat of wild and bred animals in central Italy. Food Control 30 (1), 272–279. https://doi.org/10.1016/j.foodcont.2012.07.038.

National Reserach Council, 1999. Risk Assessment of Radon in Drinking Water. The National Academies Press, Washington DC. https://doi.org/10.17226/6287.

Niede, R., Benbi, D.K., 2022. Integrated review of the nexus between toxic elements in the environment and human health. AIMS Public Health 9 (4), 758–789. https://doi.org/10.3934/publichealth.2022052, 30.

Pacella, A., Cremisini, C., Nardi, E., Montereali, M.R., Pettiti, I., Giordani, M., Mattioli, M., Ballirano, P., 2018. Different erionite species bind iron into the structure: a potential explanation for fibrous erionite toxicity. Minerals 8 (2), 36. https://doi.org/10.3390/min8020036.

Paschoa, A.S., Steinhäusler, F., 2010. Technologically enhanced natural radiation. ISBN: 978-0-08-044936-4. In: Baxter, M. (Ed.), Radioactivity in the Environment, Series, 17. Elsevier Ltd., pp. 29–85

Persson, B.R., Holm, E., 2011. Polonium-210 and lead-210 in the terrestrial environment: a historical review. J. Environ. Radioact. 102 (5), 420–429. https://doi.org/10.1016/j.jenvrad.2011.01.005.

Peruzzi, F., Belvederi, G., Garberi, M.L., Giordani, M., 2016. Caratterizzazione idrogeochimica delle acque della miniera di Perticara. In: GESSI E SOLFI DELLA ROMAGNA ORIENTALE. Memorie dell'Istituto Italiano di Speleologia, s. II, 31, pp. 347–354.

Petermann, E., Bossew, P., Hoffmann, B., 2022. Radon hazard vs. radon risk-on the effectiveness of radon priority areas. J. Environ. Radioact. 244, 106833. https://doi.org/10.1016/j.jenvrad.2022.106833.

Petriglieri, J.R., Laporte-Magoni, C., Salvioli-Mariani, E., Ferrando, S., Tomatis, M., Fubini, B., Turci, F., 2021. Morphological and chemical properties of fibrous antigorite from lateritic deposit of New Caledonia in view of hazard assessment. Sci. Total Environ. 777, 146185. https://doi.org/10.1016/j.scitotenv.2021.146185.

Price, W.R., 2021. Mining for tourists: an analysis of industrial tourism and government policy in Wales. Tour. Plan. Dev. vol. 18 (4), 435–456. https://doi.org/10.1080/21568316.2020.1829695.

Righi, S., Bruzzi, L., 2006. Natural radioactivity and radon exhalation in building materials used in Italian dwellings. J. Environ. Radioact. 88 (2), 158–170. https://doi.org/10.1016/j.jenvrad.2006.01.009.

Rinaldi, I., 1987. Perticara, la miniera di zolfo, la sua gente (Pazzini, Verucchio).

Rossi, F.P., Schito, A., Manzi, V., Roveri, M., Corrado, S., Lugli, S., Reghizzi, M., 2021. Paleo-thermal constraints on the origin of native diagenetic sulfur in the Messinian evaporites: the northern Apennines foreland basin case study (Italy). Basin Res. 33 (4), 2500–2516. https://doi.org/10.1111/bre.12566.

Roveri, M., Manzi, V., Lucchi, F.R., Rogledi, S., 2003. Sedimentary and tectonic evolution of the Vena del Gesso basin (Northern Apennines, Italy): implications for the onset of the Messinian salinity crisis. Geol. Soc. Am. Bull. 115 (4), 387–405. https://doi.org/10.1130/0016-7606(2003)115%3C0387:SATEOT%3E2.0.CO;2.

Ruggieri, G., 1970. Nota illustrativa alla Carta Geologica d'Italia alla scala 1:100.000. In: Foglio 108 Mercato Saraceno. Servizio Geologico d'Italia, Ercolano.

Sahu, P., Panigrahi, D.C., Mishra, D.P., 2016. A comprehensive review on sources of radon and factors affecting radon concentration in underground uranium mines. Environ. Earth Sci. 75, 1–19. https://doi.org/10.1007/s12665-016-5433-8.

Sampalmieri, G., Iadanza, A., Cipollari, P., Cosentino, D., Lo Mastro, S., 2010. Palaeoenvironments of the Mediterranean Basin at the Messinian hypersaline/hyposaline transition: evidence from natural radioactivity and microfacies of post-evaporitic successions of the Adriatic sub-basin. Terra Nova 22 (4), 239–250. https://doi.org/10.1111/j.1365-3121.2010.00939.x.

Seiler, R.L., Stillings, L.L., Cutler, N., Salonen, L., Outola, I., 2011. Biogeochemical factors affecting the presence of ^{210}Po in groundwater. Appl. Geochem. 26 (4), 526–539. https://doi.org/10.1016/j.apgeochem.2011.01.011.

Sierro, F.J., Ledesma, S., Flores, J.A., Torrescusa, S., del Olmo, W.M., 2000. Sonic and gamma-ray astrochronology: cycle to cycle calibration of Atlantic climatic records to Mediterranean sapropels and astronomical oscillations. Geology 28 (8), 695–698. https://doi.org/10.1130/0091-7613(2000)28%3C695:SAGACT%3E2.0.CO;2.

Smith, K.P., 1992. An Overview of Naturally Occurring Radioactive Materials (NORM) in the Petroleum Industry. https://doi.org/10.2172/10145754.

Sorcaru, I.A., 2021. Industrial tourism attractions. The case of Salt Mines in Romania. In: Annals of "Dunarea de Jos" University of Galati. Fascicle I; Economics and Applied Informatics; years XXVII, n.1/2021. https://doi.org/10.35219/eai15840409163.

Tang, B., Tong, P., Xue, K.S., Williams, P.L., Wang, J.S., Tang, L., 2019. High-throughput assessment of toxic effects of metal mixtures of cadmium (Cd), lead (Pb), and manganese (Mn) in nematode *Caenorhabditis elegans*. Chemosphere 234, 232–241. https://doi.org/10.1016/j.chemosphere.2019.05.271.

United States Environmental Protection Agency US EPA, 2009. EPA Assessment of Risks From Radon in Homes. EPA, Washington, DC (402-R-03-003).

Vaaramaa, K., Lehto, J., Ervanne, H., 2003. Soluble and particle-bound U-234, U-238, Ra-226 and Po-210 in ground waters. Radiochim. Acta 91, 21–27. https://doi.org/10.1524/ract.91.1.21.19015.

Vengosh, A., Coyte, R.M., Podgorski, J., Johnson, T.M., 2022. A critical review on the occurrence and distribution of the uranium-and thorium-decay nuclides and their effect on the quality of groundwater. Sci. Total Environ. 808, 151914. https://doi.org/10.1016/j.scitotenv.2021.151914.

Wei, C.L., Murray, J.W., 1994. The behavior of scavenged isotopes in marine anoxic environments - Pb-210 and Po-210 in the water column of the Black-Sea. Geochim. Cosmochim. Acta 58, 1795–1811. https://doi.org/10.1016/0016-7037(94)90537-1.

World Health Organization (WHO), 1999. Occupational and Environmental Health Team. Hazard Prevention and Control in the Work Environment. Report WHO/SDE/OEH/99.14, Geneva Airborne Dust.

World Health Organization (WHO), 2009. Handbook on Indoor Radon a Public Health Perspective. World Health Organization, Geneva, Switzerland.

World Health Organization (WHO), 2011. World Health Organization Guidelines for Drinking Water Quality, fourth ed. http://www.who.int/water_sanitation_health/publications/2011/dwq_guidelines/en/.

World Health Organization (WHO), 2017. Guidelines for drinking-water quality. In: Incorporating the First Addendum: Radiological Aspects, Fourth edition. World Health Organization (WHO), Geneva. https://www.ncbi.nlm.nih.gov/books/NBK442376/.